

# Surface Selective $^1\text{H}/^{29}\text{Si}$ CP NMR by NOE Enhancement from Laser Polarized Xenon<sup>1</sup>

T. Pietraß,\* R. Seydoux, and A. Pines

Materials Sciences Division, Lawrence Berkeley National Laboratory and Department of Chemistry, University of California at Berkeley, Berkeley, California 94720; and \*Department of Chemistry, New Mexico Tech, Socorro, New Mexico 87801

Received June 13, 1997; revised March 18, 1998

**The surface proton spin polarization created by the spin-polarization-induced nuclear Overhauser effect from optically polarized xenon can be transferred in a subsequent step by solid-state cross polarization to another nuclear spin species such as  $^{29}\text{Si}$ . The technique exploits the dipolar interactions of xenon nuclear spins with high  $\gamma$  nuclei such as  $^1\text{H}$ , and is experimentally simpler than direct polarization transfer from  $^{129}\text{Xe}$  to heteronuclei such as  $^{13}\text{C}$  and  $^{29}\text{Si}$ .** © 1998 Academic Press

**Key Words:** optical pumping;  $^{29}\text{Si}$  solid state NMR; spin polarization induced nuclear Overhauser effect; cross polarization.

## INTRODUCTION

Sensitivity is often a limiting factor in nuclear magnetic resonance (NMR) spectroscopy of surfaces. An approach to the selective NMR enhancement of surfaces using  $^{129}\text{Xe}$  NMR spectroscopy of interior cavities has been demonstrated in recent years (1, 2), and the technique has been extended to the study of exterior, more easily accessible surfaces by the introduction of optically polarized xenon gas (3–6). The high nuclear spin polarization of the xenon can be transferred to surface protons at low temperatures (7, 8) by solid-state Hartmann–Hahn cross polarization (CP) (9, 10), a technique that benefits from the strong dipolar coupling of protons to adsorbed xenon due to the high gyromagnetic ratio  $\gamma$  of the protons.

An alternative approach to polarization transfer from optically polarized xenon to proton spins is possible in liquids through the nuclear Overhauser effect (NOE), a mechanism dubbed spin-polarization-induced NOE (SPINOE) (11). The SPINOE was recently extended to the solid state, where proton spins in silanol groups or in polymer coatings and  $^{13}\text{C}$  enriched carbon dioxide on surfaces were spin polarized upon contact with optically polarized noble gases ( $^{129}\text{Xe}$ ,  $^3\text{He}$ ) (12).

The SPINOE technique is advantageous in materials for which the relaxation time of the observed nuclear spins is close

to the relaxation time of the adsorbed  $^{129}\text{Xe}$  and it works best for high natural abundance nuclei with high  $\gamma$  such as protons. The first limitation of relaxation times may be alleviated by continuously administering freshly polarized xenon, an approach made possible through the new generation of diode array lasers, capable of polarizing large quantities of gas (13, 14). The second limitation arises from the reduced resolution of solid-state proton NMR. Even with the application of magic angle spinning and multiple pulse sequences, the information content of  $^1\text{H}$  solid-state NMR spectra is limited. Thus, the study of nuclear spins other than those of protons is desirable.

In this work, we show that the surface proton spin polarization created by SPINOE from optically polarized xenon can be transferred in a subsequent step by conventional solid-state cross polarization to another nuclear spin species such as  $^{29}\text{Si}$ . In the following, this technique will be called SPINOE-CP. Because the xenon is in selective contact with the surface of the material, such an approach makes it possible to observe the NMR of silicon nuclei residing close to the surface. With the addition of magic angle spinning, currently under way, the resolution of different surface sites should be substantially enhanced.

## RESULTS AND DISCUSSION

A series of SPINOE experiments with  $^1\text{H}$  detection was carried out in order to check the time evolution and the maximal polarization enhancement of the spin reservoir exploited for the subsequent transfer to  $^{29}\text{Si}$ . Figure 1 shows the integrated  $^1\text{H}$  NMR signal intensities of hydroxyl protons on a silica surface, acquired with single pulse excitation and both positive and negative  $^{129}\text{Xe}$  nuclear spin polarizations. A positive (negative) NOE corresponds to an enhanced  $^1\text{H}$  signal of equal (opposite) phase with respect to the thermal Boltzmann equilibrium NMR signal. The increase (decrease) in signal intensity at  $t = 0$  (Fig. 1) for positive (negative) NOE indicates the point in time at which the xenon was admitted to the sample. The polarization of the protons ( $I$  spins) due to cross relaxation with the xenon ( $S$  spins) is described by (11)

<sup>1</sup> This work was supported by the U.S. Department of Energy DE-AC03-76SF00098. The U.S. Government's right to retain a nonexclusive, royalty-free license in and to the copyright covering this paper, for governmental purposes, is acknowledged.

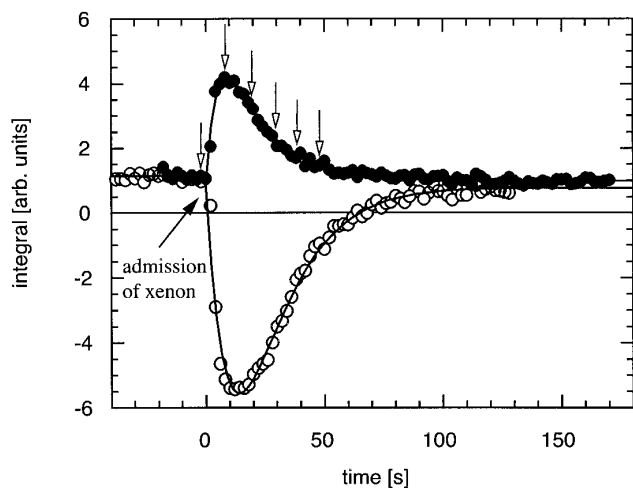


**FIG. 1.** Time dependence of the  $^1\text{H}$  NMR signal intensity of hydroxyl protons of the silica Aerosil 300 in contact with optically polarized xenon at a temperature of 135 K. A pulse duration of  $2\ \mu\text{s}$ , corresponding to a  $20^\circ$  flip angle, was applied. Individual data points are separated by a time delay of 2.0 s. Full circles represent enhanced signals with polarization of the same sign as the Boltzmann thermal equilibrium polarization and empty circles correspond to signals arising from interactions with xenon of opposite spin polarization. The proton background signal of the probe, determined to 40% in a separate experiment without sample under otherwise identical conditions, has been subtracted from the data. The admission of the xenon to the sample marks  $t = 0$  and the solid curve represents a fit to the data according to Eq. [2]. Arrows mark the times at which the CP sequence was applied in the corresponding experiments to obtain the  $^{29}\text{Si}$  NMR data of Figs. 2 and 3.

$$\frac{I_z - I_0}{I_0} = -\frac{\sigma_{IS}}{\rho_I} \frac{\gamma_S \cdot S(S+1)}{\gamma_I \cdot I(I+1)} \frac{S_z - S_0}{S_0} \quad [1]$$

where  $I_0$  and  $S_0$  are the thermal Boltzmann equilibrium polarizations of the  $I$  and  $S$  spins,  $I_z$  and  $S_z$  are the  $z$  components of the  $I$  and  $S$  spin polarizations at time  $t_0$  where  $I_z$  goes through an extremum,  $\sigma_{IS}$  is the cross relaxation rate,  $\rho_I$  is the auto-relaxation rate, and  $\gamma_I$ ,  $\gamma_S$  are the gyromagnetic ratios. The dynamics of the NOE signal are

$$I(t) = a + b \cdot (e^{-t/T_{\text{dec}}} - e^{-t/T_{\text{pol}}}), \quad [2]$$

which is obtained from the Solomon equations for the case of small cross-relaxation rates compared with the self-relaxation (15). Under ideal conditions, i.e., neglecting the dynamics of gas adsorption, the buildup ( $T_{\text{pol}}$ ) and decay ( $T_{\text{dec}}$ ) time constants of the proton spin polarization should be given by the spin lattice relaxation times of the protons and the adsorbed xenon, respectively. A fit to the data (solid line in Fig. 1) with Eq. [2] yields for the positive  $^1\text{H}$  NOE experiment the time constants  $T_{\text{pol}} = 5.6 \pm 2.4$  s and  $T_{\text{dec}} = 16.5 \pm 1.0$  s; for the negative  $^1\text{H}$  NOE experiment,  $T_{\text{pol}} = 10.4 \pm 4.0$  s and  $T_{\text{dec}} = 16.5 \pm 2.8$  s. The discrepancy in the buildup times is attributed to the small number of points defining the rising part of the NOE data.

The proton spin-lattice relaxation time was determined independently in the absence of xenon with a saturation recovery pulse sequence. The buildup of the magnetization can be described within experimental error by a monoexponential function with a time constant  $T_1 = 8.4 \pm 0.8$  s. This relaxation time agrees quite well with the time constants  $T_{\text{pol}}$  governed primarily by proton spin-lattice relaxation (12).

Compared with the thermal equilibrium signal, the enhancement factor obtained for the negative NOE was about six, and for the positive NOE it was about three. These numbers present a lower limit for the NOE on the proton spins, since part of the thermal equilibrium signal used for reference may arise from protons in sample regions not accessible to the xenon.

Figure 2a shows a series of  $^{29}\text{Si}$  NMR spectra obtained by Hartmann-Hahn cross polarization from negatively SPINOE-

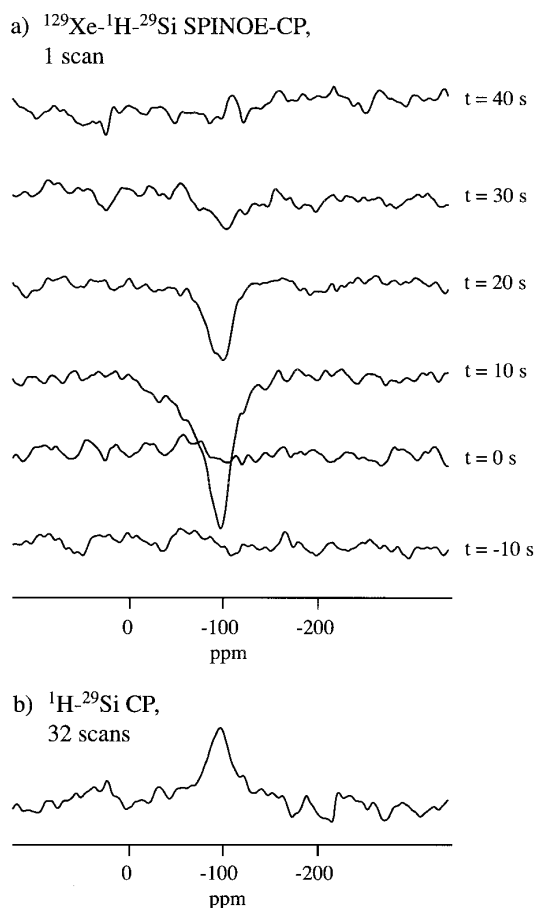


**FIG. 2.** (a) Single scan  $^{29}\text{Si}$  NMR spectra obtained with a cross polarization sequence with proton spins in contact with optically polarized xenon serving as the magnetization reservoir ( $T = 135$  K). The spin orientation of the xenon corresponded to a negative NOE on the protons. The admission of the xenon occurred right after acquisition of the spectrum marked  $t = 0$ . A residual background signal, determined by a control run without polarized xenon under otherwise identical conditions, was subtracted from the spectra. (b) Conventional  $^1\text{H}/^{29}\text{Si}$  CP NMR signal after 32 accumulated scans recorded at the same temperature with a recycle delay of 2 s, which restored only 30% of the proton polarization. The duration of the contact pulse was 5 ms (a, b).

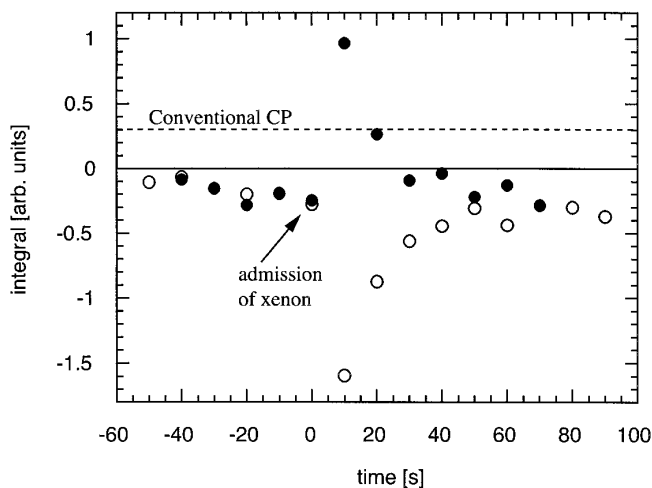


**FIG. 3.**  $^{29}\text{Si}$  NMR signal intensities obtained from spectra recorded under the conditions shown in Fig. 2a for positive (full circles) and negative (empty circles) NOE on the protons. Individual data points are separated by a time delay of 10.0 s. The admission of the xenon occurred immediately after the point marked  $t = 0$ . The dashed line marked “Conventional CP” denotes the signal intensity of a single CP scan without the effect of SPINOE-CP, obtained by scaling a spectrum of 32 transients, accounting for the number of scans and the repetition time.

polarized proton spins. The phase of the  $^{29}\text{Si}$  NMR spectra (Fig. 2a) is thus negative with respect to the signal obtained by accumulating 32 scans (Fig. 2b) without the addition of xenon. Here, residual  $^{29}\text{Si}$  thermal Boltzmann polarization, most likely originating from the glass, is eliminated by the application of a phase cycle. For the single scan spectra of Fig. 2a, however, this residual polarization would be detectable. The spectra shown in Fig. 2a are therefore presented as the difference of the signal in the experiment using polarized xenon and the control experiment without xenon. Hence, no signal is observable before the admission of the xenon, and the evolving peak is due solely to SPINOE-CP transfer.

The time dependence of the  $^{29}\text{Si}$  NMR integrated signal intensity for both positive and negative NOE is depicted in Fig. 3. Here, the data have not been corrected by subtraction of the control experiment, giving rise to a small baseline offset originating from the residual Boltzmann equilibrium signal. This residual polarization is larger than the one arising from a single CP scan without NOE enhancement. The time constants for the decay of the signal, expected to be the same as that measured for the SPINOE-induced proton polarization (Fig. 1), were  $10.8 \pm 2.2$  s (positive NOE) and  $11.8 \pm 1.3$  s (negative NOE). These values are slightly lower than those for the proton spin polarization decay, but the difference is not considered significant in view of the small number of data points.

The enhancement factor for the  $^{29}\text{Si}$  NMR signal was determined from comparison with the conventional CP signal after accumulating 32 scans. The CP spectrum (Fig. 2b) was recorded with a 2-s delay between transients, restoring only 30% of the equilibrium proton spin polarization, and was therefore

scaled to a single scan at 100% original proton magnetization, indicated by the dashed line in Fig. 3. The enhancement factors are four for the positive and five for the negative NOE. These values lie within the range obtained for the proton NOE enhancement, indicating that a large fraction of the proton spins relevant for CP to  $^{29}\text{Si}$  were in contact with the polarized xenon. These results make the study of other low  $\gamma$  species with typically long spin-lattice relaxation times, such as  $^{13}\text{C}$ ,  $^{77}\text{Se}$ ,  $^{113}\text{Cd}$ , etc., quite promising.

The spectra depicted in Fig. 2 show only one featureless peak, as may be expected from a solid-state  $^{29}\text{Si}$  NMR signal at low magnetic field and in the absence of magic angle spinning. The chemical shift corresponds to the range common for Si-O species. The full line width at half maximum is about 1 kHz or 28 ppm. Linewidths and shifts correspond to the values reported in the literature (16), where magic angle spinning at  $\approx 3$  kHz allowed the resolution of shoulders indicating the presence of  $\text{Q}^2$ ,  $\text{Q}^3$ , and  $\text{Q}^4$  silicon-oxygen tetrahedra.

A direct transfer of the xenon polarization to silicon nuclear spins was attempted, but yielded no observable enhancement. Apparently either the silicon atoms are located far from surface sites accessible to the xenon or their relaxation time is very long compared with the decay of xenon spin polarization. For surface spin species with long relaxation times the direct SPINOE is less favorable than the route via protons or other high abundant, high  $\gamma$  nuclei such as  $^{31}\text{P}$  or  $^{19}\text{F}$ , as a large fraction of the xenon polarization is lost comparatively rapidly due to other relaxation processes such as interaction with paramagnetic centers or chemical shift anisotropy. Whereas the NOE is a stochastic low-probability process that is effective for any spin species present, Hartmann-Hahn cross polarization can be carried out selectively to the desired nuclear isotope. Long internuclear distances can be accounted for to a certain extent by variation of the contact pulse length. Although the silicon atoms, bonded to hydrogen via oxygen, are too far away from the surface for direct polarization transfer from the xenon, our experiments show that the silicon can be polarized indirectly from protons located at the outermost regions of the material where xenon accessibility is most facile. The Hartmann-Hahn cross polarization sequence can be replaced, for adequate systems, by other methods such as adiabatic passage (10, 17), or supplemented by selectivity enhancing sequences such as dipolar dephasing (18).

## CONCLUSIONS

In summary we have demonstrated that cross polarization from SPINOE-enhanced surface proton spins to other surface nuclear spin species is feasible. Despite the moderate enhancement factors of about fivefold over conventional CP, the strength of the presented method lies in the surface selectivity. Nevertheless, the enhancement factors obtained are sufficiently encouraging to propose this technique as a general approach to the study of surfaces where high  $\gamma$  nuclei, readily polarized at

low temperatures through contact with optically polarized xenon, are available as a magnetization source for less abundant nuclei. The SPINOE-CP experiment yields additional information about connectivities of surface atoms. In order to enhance the resolution, the implementation of magic angle spinning is currently under way.

### EXPERIMENTAL

NMR experiments were carried out on a Chemagnetics (Otsuka Electronics) spectrometer at a magnetic field of 4.2 T in a home-built, double-tuned probe capable of low-temperature operation. The sample was contained in an L-shaped sample tube, whose long neck extended through the length of the NMR probe. Outside the probe, the neck was equipped with a valve, connections to a vacuum manifold, and the xenon gas reservoir. The dewared sample region was cooled by a flow of nitrogen gas. Careful thermal insulation of the sample region and purging of the capacitors (situated directly underneath the dewared region) with hot air allowed operation at temperatures as low as 110 K for several hours.

The Hartmann-Hahn condition for  $^1\text{H}/^{29}\text{Si}$  (Larmor frequencies 178.021 and 35.364 MHz, respectively) with a conventional pulse sequence was initially set at room temperature using the resonance of kaolinite (19). Our sample, 160 mg of Aerosil 300 (Degussa Corp.), yielded a good signal to noise ratio after 32  $^1\text{H}$  to  $^{29}\text{Si}$  CP transient signals, a condition necessary for evaluating the SPINOE-CP enhancement following a single scan. After operation for 1 h at the desired temperature (135–140 K), the probe reached conditions sufficiently stable for the CP experiments. Optimal CP conditions were obtained with the same power levels as used at room temperature. The  $90^\circ$  pulse length on the proton channel was set to 9  $\mu\text{s}$ . For the hydrogen on Aerosil 300, bound to oxygen of hydroxyl groups, CP contact times of  $\approx 5$  ms were found to yield optimal NMR signals. The sample surface was cleaned by evacuation for several hours to a pressure of  $10^{-5}$  to  $10^{-6}$  torr at room temperature.

Isotopically enriched xenon (80%  $^{129}\text{Xe}$ , <2%  $^{131}\text{Xe}$ ; Cambridge Isotope Labs) was optically polarized in an apparatus described previously (4, 20) by irradiation with circularly polarized pumping light supplied by a titanium sapphire laser (Schwartz) pumped by an argon ion laser (Coherent). Typically, the power of the continuous incident light was 1.3 to 1.4 W, resulting in a spin polarization of about 6%. Opposite helicities of the pumping light result in population excesses of nuclear spin levels "up" or "down," causing a  $180^\circ$  phase shift of the NMR signals. The same effect can be achieved by changing the direction of the magnetic field housing the optical pumping cell. The latter method was used in the present experiments since it cancels phase errors due to imperfections in the arrangement and setting of the quarter wave plate.

For the SPINOE experiments, the sample was precooled and the Hartmann-Hahn condition established while the xenon was

subjected to laser polarization. Data acquisition in constant time intervals (10 s) of single transients induced by a conventional cross-polarization sequence was initiated *before* admitting xenon to the sample, in order to establish a steady state of background thermal Boltzmann polarization arising mainly from  $^{29}\text{Si}$  in the glass sample tube. The optical pumping cell, containing about 0.5 mmol xenon, was then attached to the sample chamber and the optically polarized gas admitted to the sample while data acquisition continued. The xenon vapor pressure was monitored throughout the experiment. Within a few seconds, more than 90% of the gas had been adsorbed and no further pressure drop was observed for the duration of the experiment. The aerosil surface area had been determined by the supplier using nitrogen adsorption (300  $\text{m}^2/\text{g}$ ). Assuming that one xenon atom covers roughly 20  $\text{\AA}^2$ , an excess of 30% of the amount required for monolayer coverage was achieved. Immediately upon completion of the experiment, a control experiment was undertaken under identical experimental conditions, but without further addition of xenon. This step was necessary in order to measure the background signal. Further experimental details are given in the figure captions.

### ACKNOWLEDGMENTS

This work was funded by the Director, Office of Energy Research, Office of Basic Energy Sciences, Materials Sciences Division, of the U.S. Department of Energy, under Contract DE-AC03-76SF00098. We express our gratitude to the Degussa Corporation for providing the Aerosil samples. R. S. acknowledges support by the Swiss National Science Foundation.

### REFERENCES

1. C. Jameson, A. Jameson, R. Gerald, and A. d. Dios, Nuclear magnetic resonance studies of xenon clusters in zeolite NaA, *J. Chem. Phys.* **96**, 1676 (1992).
2. C. Dybowski, N. Bansal, and T. Duncan, NMR spectroscopy of xenon in confined spaces: Clathrates, intercalates and zeolites, *Ann. Rev. Phys. Chem.* **42**, 433 (1991).
3. W. Happer, E. Miron, S. Schaefer, D. Schreiber, W. A. v. Wijngaarden, and X. Zeng, Polarization of the nuclear spins of noble-gas atoms by spin exchange with optically pumped alkali-metal atoms, *Phys. Rev. A* **29**, 3092 (1984).
4. T. Pietraß and H. C. Gaede, Optically polarized  $^{129}\text{Xe}$  in NMR spectroscopy, *Adv. Mater.* **7**, 826 (1995).
5. D. Raftery, L. Reven, H. Long, A. Pines, P. Tang, and J. A. Reimer, Spin polarized  $^{129}\text{Xe}$  NMR study of a polymer surface, *J. Phys. Chem.* **97**, 1649 (1993).
6. T. Pietraß, A. Bifone, and A. Pines, Adsorption properties of porous silicon characterized by optically enhanced  $^{129}\text{Xe}$  NMR spectroscopy, *Surf. Sci.* **334**, L730 (1995).
7. H. W. Long, H. C. Gaede, J. Shore, L. Reven, C. R. Bowers, J. Kritzenberger, T. Pietraß, A. Pines, P. Tang, and J. A. Reimer, High-field cross polarization NMR from laser-polarized xenon to a polymer surface, *J. Am. Chem. Soc.* **115**, 8491 (1993).
8. H. C. Gaede, Y.-Q. Song, R. E. Taylor, E. J. Munson, J. A. Reimer, and A. Pines, High-field cross polarization NMR from laser-polarized xenon to surface nuclei, *Appl. Magn. Res.* **8**, 373 (1995).

9. S. R. Hartmann and E. L. Hahn, Nuclear double resonance in the rotating frame, *Phys. Rev.* **128**, 2042 (1962).
10. A. Pines, M. G. Gibby, and J. S. Waugh, Proton-enhanced NMR of dilute spins in solids, *J. Chem. Phys.* **59**, 569 (1973).
11. G. Navon, Y.-Q. Song, T. Róom, S. Appelt, R. E. Taylor, and A. Pines, Enhancement of solution NMR and MRI with laser-polarized xenon, *Science* **271**, 1848 (1996).
12. T. Róom, S. Appelt, R. Seydoux, and A. Pines, Enhancement of surface NMR by laser-polarized noble gases, *Phys. Rev. B* **55**, 11604 (1997).
13. W. J. Cummings, O. Häusser, W. Lorenzon, D. R. Swenson, and B. Larson, Optical pumping of Rb vapor using high-power  $\text{Ga}_{1-x}\text{Al}_x\text{As}$  diode laser arrays, *Phys. Rev. A* **51**, 4842 (1995).
14. B. Driehuys, G. D. Cates, E. Miron, K. Sauer, D. K. Walter, and W. Happer, High-volume production of laser-polarized  $^{129}\text{Xe}$ , *Appl. Phys. Lett.* **69**, 1668 (1996).
15. I. Solomon, Relaxation processes in a system of two spins, *Phys. Rev.* **99**, 559 (1955).
16. V. V. Brei,  $^{29}\text{Si}$  solid-state NMR study of the surface structure of aerosil silica, *J. Chem. Soc. Faraday. Trans.* **90**, 2961 (1994).
17. S. Hediger, B. H. Meier, and R. R. Ernst, Adiabatic passage Hartmann–Hahn cross polarization in NMR under magic angle sample spinning, *Chem. Phys. Lett.* **240**, 449 (1995).
18. M. Alla and E. Lippmaa, High resolution broad line  $^{13}\text{C}$  NMR and relaxation in solid norbornadiene, *Chem. Phys. Lett.* **37**, 260 (1976).
19. J. Rocha and J. Klinowski, Kaolinite as a convenient standard for setting the Hartmann–Hahn match for  $^{29}\text{Si}$  CP/MAS NMR of silicates, *J. Magn. Reson.* **90**, 567 (1990).
20. D. Raftery, H. Long, T. Meersmann, P. J. Grandinetti, L. Reven, and A. Pines, High-field NMR of adsorbed xenon polarized by laser pumping, *Phys. Rev. Lett.* **66**, 584 (1991).